Modeling of long High Voltage AC Underground

Gudmundsdottir, Unnur Stella; Bak, Claus Leth; Wiechowski, W. T.

Published in:
Proceedings of the Danish PhD Seminar on Detailed Modelling and Validation of Electrical Components and Systems 2010

Publication date:
2010

Document Version
Publisher's PDF, also known as Version of record

Modeling of long High Voltage AC Underground Cables

U. S. Gudmundsdottir , C. L. Bak and W. T. Wiechowski

ABSTRACT

THIS paper presents the work and findings of a PhD project focused on accurate high frequency modelling of long High Voltage AC Underground cables. The project is cooperation between Aalborg University and Energinet.dk. The objective of the project is to investigate the accuracy of most up to date cable models, perform highly accurate field measurements for validating the model and identifying possible disadvantages of the cable model. Furthermore the project suggests and implements improvements and validates them against several field measurements. It is shown in this paper how a new method for calculating the frequency dependent cables impedance greatly improves the modeling procedure and gives a highly accurate result for high frequency simulations.

I. INTRODUCTION

Interest towards using underground high voltage (HV) cables in power transmission has increased considerably. In order to research the possibility of using large HV AC cable systems, it is necessary to have precise simulation models.

The usual practice for validating a cable model has been to compare the simulation results with frequency domain calculations transformed to the time domain by use of Inverse Fast Fourier Transform (IFFT). This, however, does not ensure the accuracy of the entry parameters of the modeling procedure (e.g. geometry), the parameter conversions, and the modeling assumptions.

Some authors have used measurement results from [1] for transient voltage comparison [2],[3]. In other papers the cable model validation has been obtained by simulations only [4], [5]or by comparisons with field tests for cables with few or no cross bondings and with grounding of the sheath only at the cable ends [6],[7].

This paper describes modelling and high frequency simulation of a cable system and different types of validating the model. For the validation process the paper mentions measurements on two different cable systems, both cross bonded and non crossbonded cables. Furthermore the paper also points out drawbacks and improvements for long HV AC cable models. For high frequency studies, the frequency dependent phase model in EMTDC/PSCAD is used for modelling [4].

This work was supported by Energinet.dk.

U.S.G. is a PhD student at the Institute of Energy Technology, Aalborg University, 9220 Aalborg, Denmark (e-mail: usg@energinet.dk, phone no. +45 31 18 41 39).

C.L.B. is with the Institute of Energy Technology, Aalborg University, 9220 Aalborg, Denmark (clb@iet.aau.dk).

W.T.W. is with Energinet.dk, 7000 Fredericia, Denmark (WWI@energinet.dk)

Paper submitted to the PhD Seminar on Detailed Modelling and Validation of Electrical Components and Systems 2010 in Fredericia, Denmark, February 8th, 2010

II. MODELLING OF CABLES IN AN EMT-PROGRAM

A cable consists of several layers. For the common long HV AC underground cable, a single core XLPE cable is made of a core conductor, insulation, semiconductive layers, sheath conductor (also named metal screen) and an outer insulation, see Fig. 1.

Fig. 1 A typical layout of a HV XLPE cable

Impedances of a cable system are highly frequency dependent. Therefore, for high frequency transient studies, the model used should always be an EMT-program with a frequency dependent model. In such modelling, although the phase domain model is by itself known to be highly accurate, the outcome of the simulations can only be as accurate as the input parameters. Therefore, care must be taken when implementing a model for the cable. In this section, an overview over how model parameters should be chosen is given.

A. Core conductor

The purpose of the core conductor is to transmit the required current with low losses. The conductor in HV cables is either made of copper (Cu) or aluminium (Al) where Cu has a lower specific resistance. The advantage of Al over Cu, is that Al has lower mass density which leads to much less weight for the same cable capacity. For HV cables, the conductor is often stranded in order to lower the effective resistance caused by skin and proximity effect.

In most modelling software, it is only possible to model the conductor as a solid or hollow conductor. For stranded conductors the cross section is not solid and this is compensated by increasing the resistivity of the conductor. This is either done by recalculating the resistivity from the

cross sectional area and the given radius of the conductor or from the given radius and the given DC resistance of the conductor, as shown in (1). ρ is the conductor resistivity, r_1 is the conductor actual radius, A is the nominal cross sectional area of the conductor, l is the length 1 km and R_{DC} is the given DC resistance per km of the conductor.

$$\rho'_{(a)} = \rho \cdot \frac{r_1^2 \pi}{A} \quad [\Omega m] \tag{1a}$$

$$\rho'_{(b)} = R_{DC} \cdot \frac{r_1^2 \pi}{l} \quad [\Omega m] \tag{1b}$$

The material resistivity is ρ and the corrected resistivity is $\rho'_{(a)}$ and $\rho'_{(b)}$.

B. Inner insulation and SC screens

The purpose of the insulation is to ensure no electrical connection between the two current carrying components of the cable, the conductor and the sheath.

The SC screens are placed between the insulation and the conductor and again between insulation and the sheath. The purpose of the SC screens is to reduce the electrical stress in the inner insulation and prevent formation of voids between either core conductor or sheath and insulation due to bending of the cable or other mechanical stress.

It is not possible to model the semiconductive layers directly. Instead, their influence is included when modelling the insulation. The diameter of the insulation is expanded to include the semiconductive layers, and the permittivity is increased as shown in (2).

$$\varepsilon = \varepsilon_{ins} \cdot \frac{\ln(r_2 / r_1)}{\ln(b / a)} \tag{2}$$

ε_{ins} is the relative permittivity of the insulation, b and a are the outer and inner radius of the insulation and r_2 and r_1 are the inner radius of the sheath and the outer radius of the conductor, respectively.

In most EMT-programs it is only possible to represent the cable conductors by coaxial shells, both for the core and the screen. In reality, the metallic screen is made of a thin Al foil and Al or Cu wires that are helically wounded around the outer semiconductive layer. The associated axial magnetic field will cause a "solenoid effect" which increases the total inductance. The flux density B_{sol} caused by this solenoid effect is approximately given by the expression (3a) where $\mu_{ins,r}$ is the relative permeability of the insulation and N is the number of turns per meter of the cable. The associated inductance is given by (3b).

$$B_{sol}(r) = \mu_{ins,r} \mu_0 NI \tag{3a}$$

$$L = \mu_{ins,r} \mu_0 N^2 \pi (r_2^2 - r_1^2) \tag{3b}$$

In order to include the solenoid effect in the coaxial modes of propagation, the relative permeability of the main insulation is set larger than unity by the expression (4) where μ_{ins}=1.

$$\mu_{ins,r} = \mu_{ins,r} + \frac{\mu_{ins,r}}{\ln(r_2 / r_1)} \cdot 2\pi^2 N^2 (r_2^2 - r_1^2) \tag{4}$$

C. Cable sheath

The purpose of the cable sheath is to have a metallic covering used as an electrostatic screening as well as a return path for the cable's charging current and a conduction path for earth fault current in the case of a fault on the cable.

As shown in Fig. 1, for XLPE cables, the sheath consists of several layers. The two conducting sheath layers, the wired sheath layer and the laminate layer, are separated by a SC layer and are directly connected together both at each junction and cable ends.

The laminate layer is included for water resistance. The swelling tape between the wired sheath layer and the laminate layer is SC in order to ensure no potential difference between the two conducting sheath layers in the occurrence of a failure on the cable. The two conducting layers are not touching each other in order to protect the laminate from mechanical stress because of bending and for thermal protection as the laminate can not tolerate more than 180°C while the wired sheath layer can be up to 250°C.

It is a common practise when modelling the sheath in EMT-based software, to model it as a single solid hollow conductor with the resistivity doubled [8].

D. Outer insulation

The purpose of the cable outer coverings is mechanical protection against the surroundings. For XLPE cables, the outer insulation is made of high density polyethylene. The permittivity of polyethylene is 2.3, which is used for modelling the outer insulation.

E. Cross bonding points

Long cables are divided into segments with cross bondings and sheath groundings. Each minor section is approximately 1km long and two minor sections are connected with sheath crossbonding and sometimes conductor transposition as well. Each major section has three minor sections and a grounding of sheath at each end.

When modeling a long cable line for high frequency studies, each cable segment and cross bonding is modeled separately. The cross bonding is placed underground, approximately 1 m from the centre of the junction. Often Cu wires are used to perform both the cross bonding and grounding of the sheaths; the inductance in such a wire is normally estimated to be 1 μH per meter.

The grounding point for the sheaths is often placed in a box, standing on top of the ground. The distance between the box and the HV cables is approximately 10 m, represented by a 10 μH inductance.

III. Cable Impedances and Wave Propagation

For a long HV/EHV transmission cable, the electrical

properties of the cable can not be correctly explained by using simple lumped parameters. The cable should instead be explained as a series connection of many line elements of a differential length *dx* as is shown in Fig. 2, or by using wave characteristics.

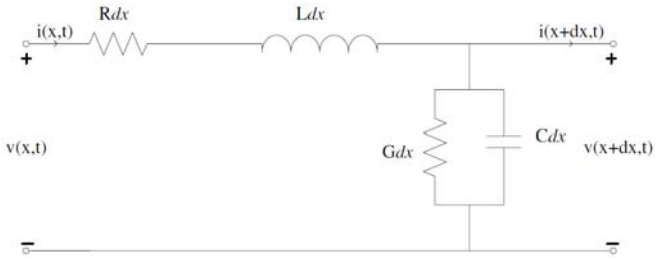

Fig. 2 Equivalent circuit of a differential length *dx* cable elements for one cable, without mutual coupling to other cables

By applying Kirchhoff's voltage law on the equivalent circuit in Fig. 2 the voltage *v(x, t)* can be found and by using Kirchhoff's current law the current *i(x, t)* can be found. If the differential length *dx* is considered infinitely small and by using frequency dependence, the time-harmonic transmission-line equation can be derived (5).

$$\begin{aligned}\frac{\partial}{\partial x}(V(x,\omega)) &= [Z(\omega)]\cdot(I(x,\omega)) \\ \frac{\partial}{\partial x}(I(x,\omega)) &= [-Y(\omega)]\cdot(V(x,\omega))\end{aligned} \tag{5}$$

The wave characteristic method is based on (5) where series connection of many line elements of length *dx* represent the transmission cable. This method is used to solve for *V(x,ω)* and *I(x,ω)* by combining the current and voltage derivatives in (5) and introducing the complex propagation constant γ. This gives the cable's terminal conditions (6).

$$\begin{aligned}\frac{\partial^2}{\partial x^2}V(x,\omega) &= \gamma^2 V(x,\omega) \\ \frac{\partial^2}{\partial x^2}I(x,\omega) &= \gamma^2 I(x,\omega) \\ \gamma &= \sqrt{[Z]\cdot[Y]} = \alpha + j\beta\end{aligned} \tag{6}$$

Where α is the wave attenuation and β is the phase constant, containing the wave velocity.

For investigating the wave propagation and solving the cable's terminal conditions, the cables impedance and admittance must be calculated. This is done in all cable models and is often referred to as the cable constant calculations.

A. Cable impedance calculations

For analyzing the series impedance matrix of the cable, the internal loops of each cable are considered, see Fig. 3. The first loop is formed by the core conductor with the sheath as return and the second loop is formed by the sheath with the ground as return [9].

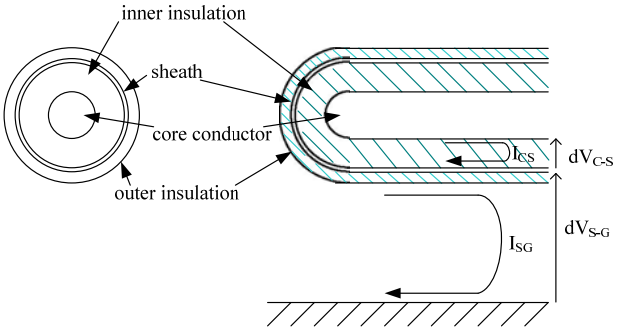

Fig. 3 Current loops in a single core coaxial cable. ICS is the current in the loop formed by core conductor with sheath as return, ISG is the current in the loop formed by sheath with ground as return, dVC-S is the voltage difference between core conductor and sheath and dVS-G is the voltage difference between the sheath and ground.

From Fig. 3 the impedance equivalent circuit for three single core cables can be derived, seeFig. 4, [10].

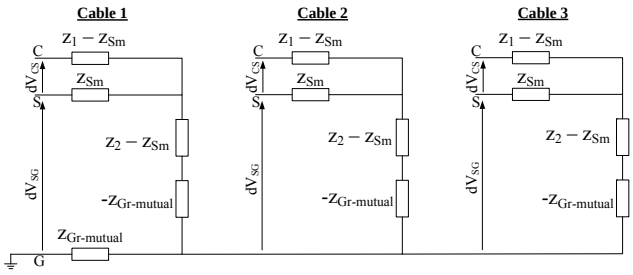

Fig. 4 Impedance equivalent circuit for the loop formation.

The phase domain impedance matrix can be constructed based on Fig. 4, where the upper case indices 1, 2, 3 refer to cable number or phases (7).

$$\begin{bmatrix} Z_{11}^1 & Z_{12}^1 & 0 & 0 & 0 & 0 \\ Z_{12}^1 & Z_{22}^1 & 0 & Z_{m12} & 0 & Z_{m13} \\ 0 & 0 & Z_{11}^2 & Z_{12}^2 & 0 & 0 \\ 0 & Z_{m12} & Z_{12}^2 & Z_{22}^2 & 0 & Z_{m23} \\ 0 & 0 & 0 & 0 & Z_{11}^3 & Z_{12}^3 \\ 0 & Z_{m13} & 0 & Z_{m23} & Z_{12}^3 & Z_{22}^3 \end{bmatrix} \tag{7}$$

Z_{12} is the mutual impedance of conductor and sheath and Z_{m12}, Z_{m13}, Z_{m23} are the mutual ground impedances between cables 1-2, 1-3 and 2-3 respectively. The impedances Z_{11} and Z_{22} are calculated by (8), [9], [11], [12],[13].

$$Z_{11} = Z_{\text{C-outer}} + Z_{\text{CS-insul}} + Z_{\text{S-inner}} \tag{8a}$$

$$Z_{22} = Z_{\text{S-outer}} + Z_{\text{SG-insul}} + Z_{\text{G}} \tag{8b}$$

Where $Z_{C\text{-}outer}$, $Z_{CS\text{-}insul}$, $Z_{S\text{-}inner}$, $Z_{S\text{-}outer}$, $Z_{SG\text{-}insul}$ and Z_G are the conductor series impedance, the inner insulation series impedance, the sheath inner series impedance, the sheath outer series impedance, the outer insulation series impedance and the earth self impedance respectively. The impedance calculations are often referred to as the Ametani equations or simply the cable constants. Cable admittance calculations

The shunt admittance matrix Y_{shunt} is somewhat simpler to

For multiple single conductor cables, there is no mutual coupling in the admittances of adjacent cables. Therefore the full phase domain shunt admittance matrix for a three cable system with three single core cables is (9)

$$\begin{bmatrix} Y_{11}^1 & -Y_{11}^1 & 0 & 0 & 0 & 0 \\ -Y_{11}^1 & Y_{22}^1 & 0 & 0 & 0 & 0 \\ 0 & 0 & Y_{11}^2 & -Y_{11}^2 & 0 & 0 \\ 0 & 0 & -Y_{11}^2 & Y_{22}^2 & 0 & 0 \\ 0 & 0 & 0 & 0 & Y_{11}^3 & -Y_{11}^3 \\ 0 & 0 & 0 & 0 & -Y_{11}^3 & Y_{22}^3 \end{bmatrix} \quad (9)$$

Y_{11} is the admittance of the cables inner insulation and Y_{22} is the sum of the admittance of inner and outer insulation (10).

$$\begin{aligned} Y_{11} &= G_{i1} + j\omega C_{i1} \\ Y_{22} &= (G_{i1} + j\omega C_{i1}) + (G_{i2} + j\omega C_{i2}) \end{aligned} \quad (10)$$

Where G_{i1}, C_{i1} and G_{i2}, C_{i2} are the shunt conductance's and capacitances of inner and outer insulation respectively.

IV. Field Measurements

The measurements should validate the models for transient behaviour. According to IEC 60071-2 an impulse of 1.2x50µs can be used to simulate lightning overvoltages.

The field measurements use an impulse test to validate the cable performance and model calculations for the cable terminal conditions given in (6).

A. Measurement preparation

Before starting any field tests, the measurement preparation is of great importance. Field measurements on long HV cables can not be repeated after need, as they usually are restricted in time by the utility company.

A simplified simulation model should be used for the system to be measured, both in order to plan where and what to measure as well as to have a base for comparison at the measurement site. This is done in order to make sure that all connections and instruments are working properly.

In the project presented in this paper, two different cable systems were measured with different measurement setups. First of all a three phase 400 kV 8km long 1200 mm^2 XLPE flat formation single core cable system was measured and second of all a three phase150 kV 100 km long 1200 mm^2 XLPE trefoil single core underground and pipe type sea cables were measured. This sub/underground cable system was measured during cable installation allowing for measurements both on parts of the cable and the whole cable line.

B. Field measurements on 400 kV cable system

The purpose of the field measurements on the 400 kV cable system was to analyse the cable model, investigate the accuracy of the model and use wave propagation to identify origin of disagreement between measurements and simulations.

Fig. 5 Field test facilities at each cable end of the 400 kV cable system

The 400 kV cable system is part of a longer transmission line of hybrated cable/OHLs. The cables were disconnected in both ends from the OHL. For detailed description of the measurement setup and field test method, the reader is referred to [14].

The generator used for the impulse test is a HAEFELY PC6-288.1 surge tester. It is used to generate a 4.28 kV 1.2/50µs impulse propagating into the core conductor on one of the phases. Fig. 6 shows the comparison of the measured and simulated sending end current propagating into the energised core conductor.

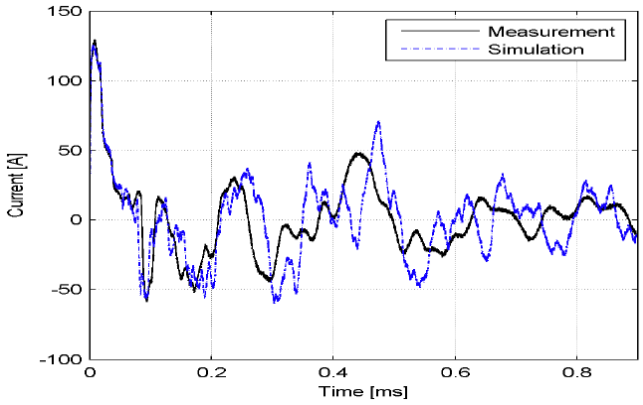

Fig. 6 Comparison of sending end current on energized core conductor

From Fig. 6 it can be seen that the current follows very closely until about 48 µs. After this, the current waves become more and more out of phase as the current becomes affected by more cross bondings, grounding points and reflected waves. Also, the sending end voltage becomes affected by incoming waves. It can also be observed in Fig. 6 how, despite deviation, some similarities between simulations and measurements, where the simulated wave appears to be less damped and delayed. This can be caused by inaccuracies in the real and imaginary parts of the characteristic admittance matrix $\boldsymbol{Y_C}$ in (11).

$$\begin{aligned} i &= Y_C v \\ Y_C &= Z^{-1}\sqrt{ZY} \end{aligned} \quad (11)$$

Where $\boldsymbol{v}$ is the vector of voltages, $\boldsymbol{Y_c}$ is the characteristic

admittance and ***i*** is the vector of currents. ***Z*** and ***Y*** are the per-unit-length series impedance and shunt admittance of the cable system. By examining the wave propagation of the sending end current in the modal domain, the reason for the deviation after 48 μs can be identified [15].

Fig. 7 Measurement instruments for cable measurements on 400 kV cable

The results for the wave propagation analysis is shown in Fig. 8. By closely examining when the disagreement between measured and simulated I_{C1} current begin, it can be noticed that this happens when the sheath currents start flowing. The reason for this is the intersheath mode, which starts flowing when sheath currents are measured.

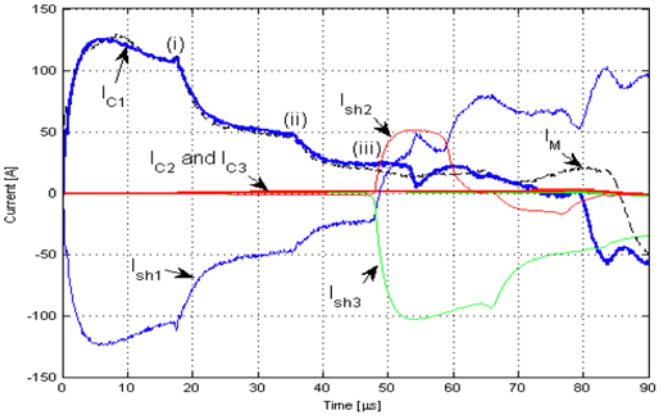

Fig. 8 Simulated phase currents. I_{c1}-I_{c3} are conductor currents, I_{sh1}-I_{sh3} are sheath currents. I_M is the measured current

Before this time, the comparison is close to perfect, which indicates a fundamentally correct model of the cable and crossbonding points, as the reflected coaxial wave does not cause deviation between measurements and simulations. Because of deviation first appearing at t=48.7 μs, it can be concluded that the model does on the other hand not correctly represent the propagation characteristics of the intersheath modes. This is not very surprising as they are strongly affected by the actual current distribution in the sheaths. The current distribution is with intersheath modes strongly dependent on proximity effects [6] which are ignored in the simulation software.

C. Field measurements on 150 kV cable system

The purpose of the field measurements on the 150 kV cable system was to verify the intersheath mode as origin of disagreement between measurements and simulations, improve the cable model and validate the improved model for long cables.

Fig. 9 Measurements performed on an open end of the 150 kV land cable

The 150 kV cable is a combination of a 58 km long underground cable and 42 km long submarine cable, connected with a single junction and operated as a single element. For verifying the origin of disagreement and improving the cable model, only one minor section of the land cable was measured. Because of no cross bonding points, it was possible to directly energise different propagation modes and therefore gain better insight in exact origin of disagreement and methods of improving the cable model. For detailed description of the measurement setup and field test method, the reader is referred to [16], [17]. For validating the improved cable model for long cables the whole cable length was measured. Due to limitations in this paper, only the one section measurements will be presented here. This is also because the whole length measurements of the 150 kV cable are similar to measurements on the 400 kV cable system.

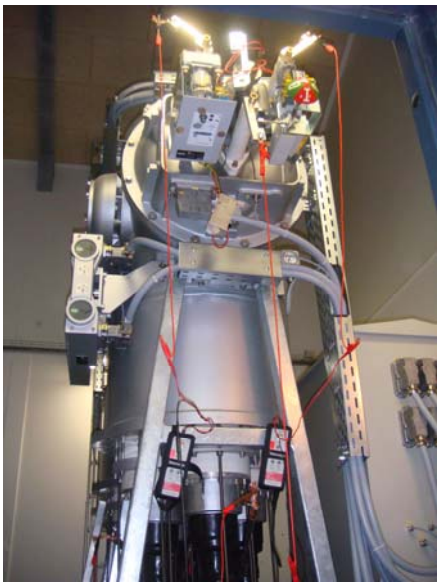

Fig. 10 Measurements on a GIS connected end of the 150 kV land cable

Fig. 11 gives the comparison of the sending end current when only the coaxial mode is energised. As indicated by the results from Fig. 8, then the coaxial mode gives almost identical comparison of simulations and measurements and it can be concluded that the propagation characteristics for the coaxial mode are accurately simulated

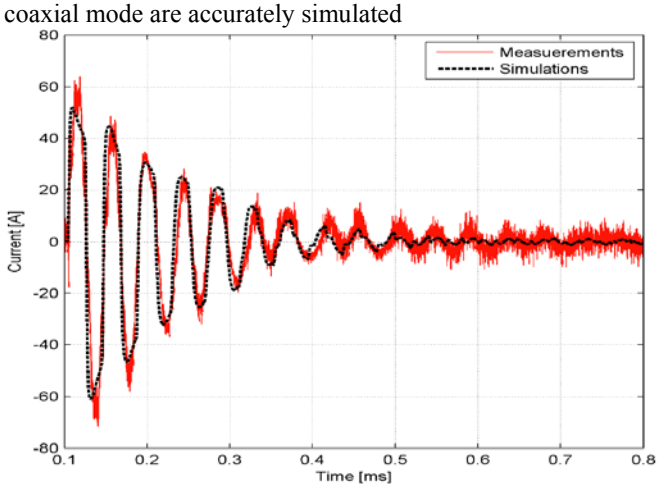

Fig. 11 Comparison of the sending end current on energised core conductor for the coaxial mode

Fig. 12 gives the comparison of the sending end current when only the intersheath mode is energised. From this figure, it is obvious that the simulation model is not accurate when the intersheath mode is included in the current propagation.

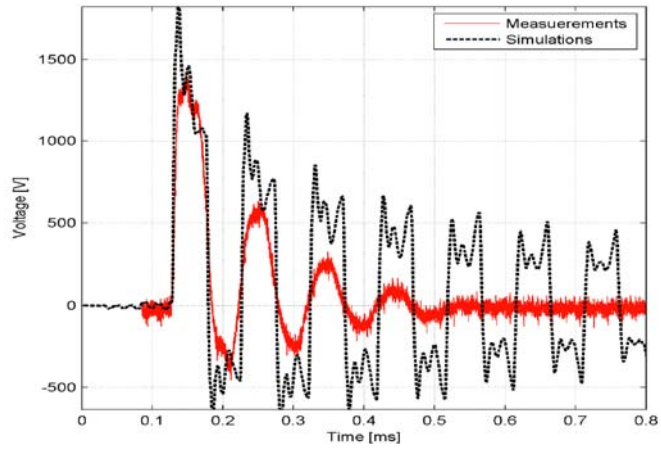

Fig. 12 Comparison of the sending end current on energised sheath conductor for the intersheath mode

As shown in Fig. 1, for XLPE cables, the sheath consists of several layers. The two conducting sheath layers, the wired sheath layer and the laminate layer, are separated by a SC layer and are directly connected together both at each junction and cable ends.

The laminate layer is included for water resistance. The swelling tape between the wired sheath layer and the laminate layer is SC in order to ensure no potential difference between the two conducting sheath layers in the occurrence of a failure on the cable. The two conducting layers are not touching each other in order to protect the laminate from mechanical stress because of bending and for thermal protection as the laminate can not tolerate more than 180°C while the wired sheath layer can be up to 250°C.

It is a common practise when modelling the sheath in EMT-based software, to model it as a single solid hollow conductor with the resistivity increased [8], [15]. This representation has been shown to be insufficient for accurate HV XLPE cable modelling [15], [16]. For improving this method and correct for this sheath representation, the sheath impedance in (8) has been split into three; impedance because of the wired sheath layer, because of the SC layer and because of the laminate layer. A more thorough description of this method can be found in [17]. The results from including such a layered sheath representation is shown in Fig. 13.

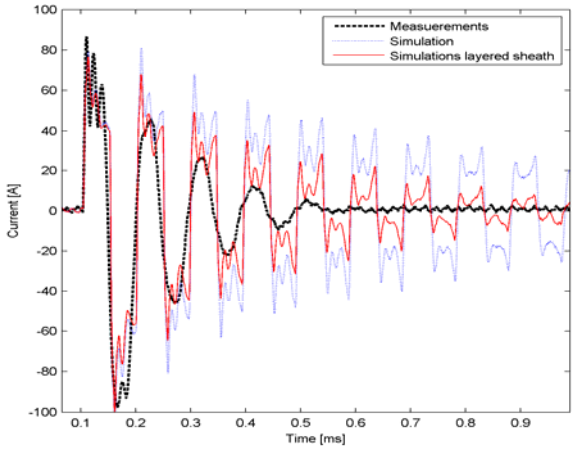

Fig. 13 Comparison of the sending end current on energised sheath when layered sheath is included.

Although improved, Fig. 13 still shows some deviation between measurements and simulation results. This is due to proximity effect which is not included in the simulation software. In fact, not a single EMT-based software includes the proximity effect when calculating the impedances of the cable. The reason for this is the method of cable constant calculations presented in (7), (8,), (9) and (10). But the Ametani equations do not include proximity effect, and yet are used always when calculating the impedances of a cable.

Because of this, in the project presented in this paper, a new method of calculating the impedance, without using the cable constant calculations, has been developed and programmed in MATLAB. This method is based on subdivision of conductors first presented as a solution for arbitrary shaped cables [18]. After calculating the impedance matrix by this new method, it is imported into EMTD/PSCAD which then uses it, instead of the cable constant calculated matrix, for the Frequency dependent phase model.

A comparison of PSCAD simulations with layered sheath included, measurements and simulations with this new method, called MATLAB simulations, is shown in Fig. 14.

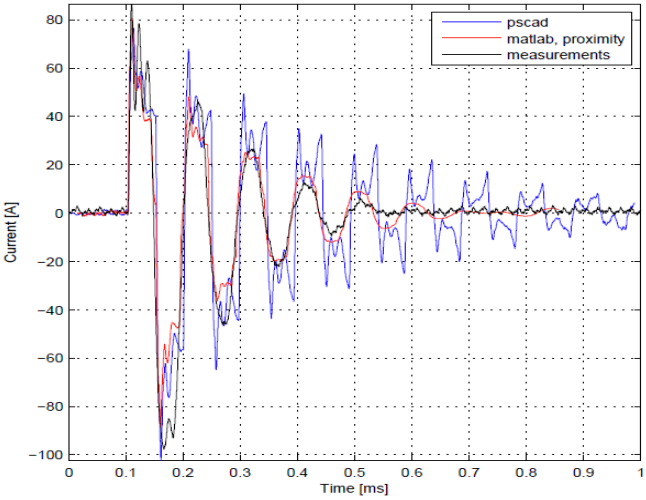

Fig. 14 Comparison of field test results, PSCAD results and new improved model with proximity effect

V. Conclusions

This paper describes modeling and high frequency simulation of a cable system and different types of validating the model. For the validation process the paper mentions measurements on two different cable systems, both cross bonded and non crossbonded cables. Furthermore the paper also points out drawbacks and improvements for long HV AC cable models. The improved modelling procedure is verified against field measurements, where the intersheath mode is explicitly excited. This is done as the presence of crossbonding points in long cables causes excitation of intersheath waves. The explicit excitation of the intersheath mode therefore verifies the model for the affect of crossbonding points in long HV AC cables, without having to take into account other modes of propagation as well.

The modelling procedure of simplifying the sheath to be represented as a single conducting coaxial layer is compared to the new method of modelling the more correct physical layout of the XLPE cable and dividing the sheath into layers. Both simulation results are compared to field measurements.

The simulations of the new modelling procedure and field test results agree quite well regarding the damping in the waveforms of the lower frequency components. This indicates that the cable model has been significantly improved. Both simulation results have though inadequate damping of high frequency transient oscillations. As the intersheath current propagates between the screens of adjacent cables, their propagation characteristics are also affected by proximity effects which are not taken into account by the simulation software when calculating the series impedance. Therefore, a new method of calculating the cable impedance matrix is introduced and verified against measurements. This method appears to give very accurate high frequency comparison of simulation and measurements, even when the intersheath mode is excited. This new method is then implemented into the EMTDC/PSCAD software. An even further advantage of this new method lies in the time for simulations. As the new method removes oscillating high frequency component in simulations, it is possible to increase the simulation step size and thereby decrease the simulation time needed.

VI. References

[1] H. Shinozaki et al, "Abnormal voltages of a core at crossbonding point," *J. Tech Lab. Chugoku Electric Power Co.*, vol. 39, pp 175-198, 1971.

[2] L. Martíl, "Simulation of transients in underground cables with frequency-dependent modal transformation matrices," *IEEE Transactions on Power Delivery*, vol. 3, no. 3, pp 1099-1110, July 1988.

[3] N. Nagaoka and A. Ametani, "Transient calculations on crossbonded cables", *IEEE Transactions on Power Apparatus and Systems*, vol. PAS-102, no. 4, pp 779-787, April 1983.

[4] A. Morched, B. Gustavsen, and M. Tartibi, "A universal model for accurate calculation of electromagnetic transients on overhead lines and underground cables," *IEEE Transactions on Power Delivery*, vol. 14, no. 3, pp. 1032-1038, July 1999.

[5] T.C. Yu and J.R. Martí, "zCable model for frequency dependent modelling of cable transmission systems," *IPST01 in Rio De Janeiro, Brazil*, paper no. IPST01-146, June 2001

[6] B. Gustavsen, J. Sletbak, and T. Henriksen, "Simulation of transient sheath overvoltages in the presence of proximity effects", *IEEE Trans. Power Delivery*, vol. 10, no. 2, pp. 1066-1075, April 1995.

[7] N. Nagaoka, T. Noda and A. Ametani, "Phase domain modelling of frequency-dependent transmission lines by means of an ARMA model", IEEE *Transactions on Power Delivery*, vol. 11, no. 1, pp. 401-411, January 1996.

[8] Gustavsen, B., 1993. A study of overvoltages in high voltage cables with emphasis on sheath overvoltages. Trondheim: NTH, Norges Tekniske Høgskole. ISBN: 82-7119-538-7.

[9] Dommel, H. W., 1996. EMTP Theory Book. 2nd ed. Vancouver: Microtran Power System Analysis Corporation.

[10] H. M. J. De Silva, "A robust multi-conductor transmission line model to simulate EM transients in underground cables," *IPST09 in Kyoto, Japan*, paper no. IPST09-175, June 2009

[11] L. M. Wedepohl, D. J. Wilcox, "Transient analysis of underground power-transmission systems," IEE Proceedings, vol. 120, no. 2, pp. 253-260, February 1973.

[12] G. Gaba, O. Saad and M. Giroux, "A closed-form approximation for ground return impedance of underground cables," IEEE Transactions on Power Delivery, vol. 11, no. 3, pp. 1536-1545, July 1996.

[13] A. Ametani, "A general formulation of impedance and admittance of cables," IEEE Transactions on Power Apparatus and Systems, vol. PAS-99, no. 3, pp. 902-910, May/June 1980.

[14] U.S. Gudmundsdottir, C. L. Bak, W. Wiechowski, K. Søgaard and M. R. Knardrupgård, "Measurements for validation of high voltage underground cable modelling," *IPST09 in Kyoto, Japan*, paper no. IPST01-15, June 2009.

[15] U.S. Gudmundsdottir, B. Gustavsen, C.L. Bak, W. Wiechowski and F.F. da Silva, "Field test and simulation of a 400 kV crossbonded cable system," *IEEE Transactions on Power Delivery*, unpublished, manuscript submitted in October 2009

[16] U.S. Gudmundsdottir, C.L. Bak, W. Wiechowski and F.F. da Silva, " Wave propagation and benchmark measurements for cable model validation," *IEEE Transactions on Power Delivery*, unpublished, manuscript submitted in November 2009

[17] U.S. Gudmundsdottir, J. De Silva, C.L. Bak and W. Wiechowski, " Double Layered Sheath in Accurate HV XLPE Cable Modeling," *IEEE PES GM 2010*, unpublished.

[18] P. de Arizon and H.W. Dommel, "Computation of cable impedances base don subdivision of conductors," *IEEE Transactions on Power Delivery*,vol. PWRD-2, no. 1, pp. 21-27, January 1987.